10.1049/iet-est.2016.0060

Characterization of the Electric Drive of EV: On-road versus Off-road Method

Clément Dépature[1,2,3], Walter Lhomme[1,3]*, Alain Bouscayrol[1,3], Loïc Boulon[2], Pierre Sicard[2], Tommi Jokela[1,4]

[1]Lille 1 University, L2EP, Lille, France
[2]Université du Québec à Trois-Rivières, GRÉI, Trois-Rivières, Canada
[3]French network on EVs and HEVs, MEGEVH, France
[4]Aalto University, Espoo, Finland
*Corresponding author: Walter.Lhomme@univ-lille1.fr

Abstract: For system design, analysis of global performance and energy management of electric vehicles, it is common to use the efficiency map of electric traction drive. The characterization of the efficiency map with high accuracy is then an important issue. In this paper an on-road method and an off-road method are compared experimentally to determine the efficiency map of electric drive of electric vehicles. The off-road method requires a dedicated experimental test bed, which is expensive and time-consuming. The on-road method is achieved directly in-vehicle. Experimental data, recorded during an on-road driving cycle, are used to determine the efficiency map using non-intrusive measurements from GPS antenna, voltage and current sensors. A versatile experimental setup is used to compare both methods on the same platform. A maximal efficiency difference of 6% is achieved in most of the torque-speed plane. It is shown that, in an energetic point of view, both methods yield similar results.

1 Introduction

The automotive industry is currently undergoing major changes due to the drawbacks related to internal-combustion powered vehicles. The main issues are greenhouse gas emissions and dependency on limited oil resources [1], [2]. New technologies such as electric, hybrid and fuel cell vehicles have been proposed and are being widely developed. Electric propulsion through an electric traction drive therefore represents a solution for low emission transportation [3], [4].

Simulation is a key issue in the development of new vehicles to benchmark, strengthen, and retrofit them [5], [6]. The United States Environmental Protection Agency is, for example, working on a full vehicle simulation model to measure the effective contributions from new technologies [7]. However, to simulate vehicles with accuracy reliable models of the different components are required. Steady-state models are classically used for system design [6], [8], analysis of global performances [9], [10] and energy management [6], [11], [12]. Steady-state models consider that all transient states are negligible. They require a low computation time and are based on experimental data by efficiency maps (look-up tables) [13]. The steady-state model of the electric traction drive [14], [15], which includes the electric machine, the power converter and their control, uses an efficiency map defined by iso-efficiency lines in the torque-speed plane [16].

Most of the steady-state models are determined separately off-road with good accuracy [17]. In this way, the IEEE 112, the IEC 60349-2 and the CSA C390-93 are the most adopted standards for electric motors [21]-[23]. For all these standards, the instrumentation accuracy, the methodology and the testing procedures are subject to specific regulations such as thermal equilibrium conditions. Minor differences may then appear depending on the standard used. Nevertheless, the off-road characterization of stand-alone components is time-consuming and expensive due to the need of dedicated experimental setups [18]. To characterize the electric traction drive an experimental setup using a load electric drive is required [15], [19]-[21]. Furthermore, the stand-alone components have to be tested outside of the vehicle. The components have then to be removed from the vehicle. After it has been characterized the electric drive is remounted in-vehicle with the risk of damage. The on-board constraints of the vehicle, like the temperature or the electromagnetic compatibility of the devices near to the tested stand-alone components, cannot also be taken into account.

To tackle these issues, other methods are developing for characterization directly in-vehicle. The actual methods are composed of extensive tests on specific rolling test benches (chassis dynamometers). Additional measurements are classically used in-vehicle to characterize the components of the vehicle like the electric drive [24], [25], the internal combustion engine [26] or the transmission [27]. When it is accessible, the on-board CAN messages can also be directly used to extract data and define the model of components [18]. Nevertheless, even if the tests are performed in-vehicle, all of these determination procedures are characterized off-road with a specific costly chassis dynamometer.

To avoid the use of a chassis dynamometer a new in-vehicle and on-road method has been proposed in [28]. From a real driving cycle the efficiency map of the electric traction drive is characterized using non-intrusive measurements from GPS antenna, voltage and current sensors. The torque of the electric drive is estimated from the parameters of the vehicle and the additional measurements. The on-road method has been applied successfully and validated to a commercial Electric Vehicle (EV), the Tazzari Zero [29].

The objective of this paper is to compare experimentally the stand-alone off-road and the new on-road method to determine the efficiency map of electric traction drive of EVs. As the off-road method is the reference in the literature, it is used as reference in this paper. In section II, the on-road and off-road methods are presented, with their application to a real commercial EV. In section III, both methods are applied to a versatile experimental setup. Finally the accuracy and limitation of the methods are discussed in section IV.

2 Characterization of the electric drive of a commercial EV

2.1 Studied vehicle

The studied traction system of the EV is composed of a battery, a Voltage-Source-Inverter (VSI), a three-phase induction machine, a gearbox, a mechanical differential and two driven wheels (Fig. 1*a*). To introduce the on-road and off-road methods, a global model of the vehicle and its control are first developed. As the paper deals with efficiencies, energetic models are sufficient in this work. The equations of the vehicle model are summarized under Table 1. All the variables are listed in Table 4 and Table 5 in the appendix. The complete model of the vehicle is detailed in [28].

Table 1. *Mathematical model of the electric vehicle*

Battery	$u_{dc} = u_0\left(SoC\right) - R_{bat} i_{ed}$	(1)
Electric drive	$\begin{cases} T_{ed} = T_{ed-ref} \\ P_m = T_{ed}\Omega_{ed} = u_{dc} i_{ed}\, \eta_{ed}\left(T_{ed}, \Omega_{ed}\right) \end{cases}$	(2)
Equivalent wheel (“bicycle model”)	$\begin{cases} F_{trac} = \left(k_{gb}/r_{wh}\right) T_{ed} \eta_{gb}^{\beta} \\ \Omega_{ed} = \left(k_{gb}/r_{wh}\right) v_{ev} \end{cases}$ with $\beta = \begin{cases} 1 \text{ when } P_m \geq 0 \\ -1 \text{ when } P_m < 0 \end{cases}$	(3)
Chassis	$F_{tot} = F_{trac} + F_{mb}$	(4)
	$M \dfrac{d}{dt} v_{ev} = F_{tot} - F_{res}$	(5)
Environment	$F_{res} = 0.5 \rho A C_x v_{ev}{}^2 + Mg\left(\sin\alpha + f_r\right)$	(6)

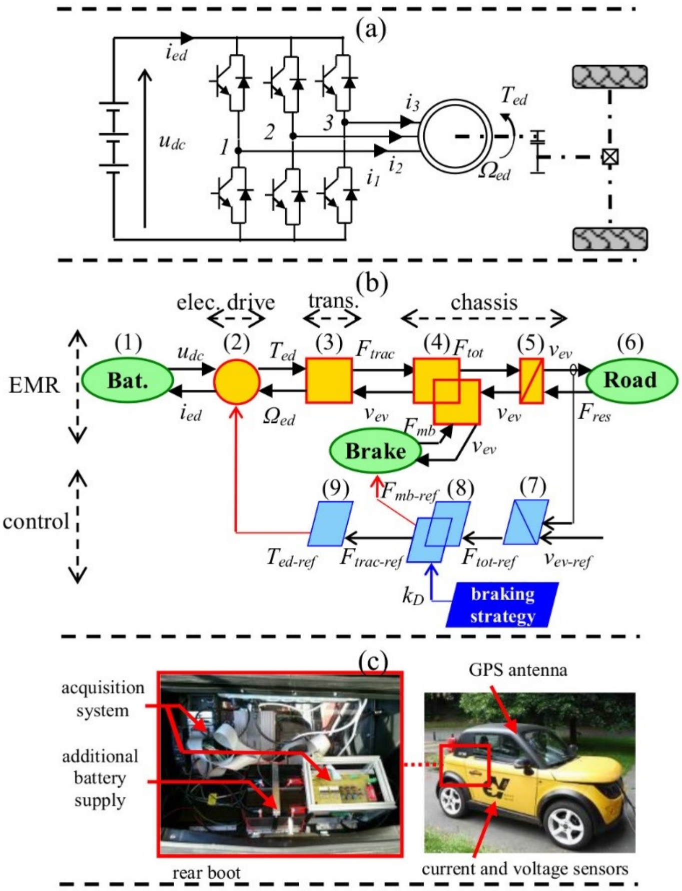

Fig. 1 *Studied traction system of an electric vehicle*

a Architecture
b EMR and control
c Tazzari Zero and supplementary sensors into the rear boot

Let us focus on the electric drive model, which is composed of the VSI, the induction machine and the associated control (a torque control is considered). With a steady-state model, it is assumed that the generated torque T_{ed} is equal to its reference $T_{ed\text{-}ref}$ [30]. Moreover, the mechanical power P_m is expressed from the electrical power through the efficiency η_{ed} from (2).

As the efficiency depends on the operating point, a look-up table generally expresses the efficiency η_{ed} from the torque T_{ed} and the rotation speed Ω_{ed} to determine the current of the electric drive i_{ed}, i.e. the input current of the VSI [14]-[16].

The models are interconnected using Energetic Macroscopic Representation (EMR). By a systemic approach, the objective of EMR is to establish a functional description of an energetic system for its control [31]. It describes the energy exchange between components of a system following the causality principles. The system is decomposed into basic subsystems in interaction (cf. Table 6 of the appendix): energy sources, accumulation elements, conversion elements and coupling elements for energy distribution. Many electric and hybrid vehicles have been studied using EMR [12], [32]-[35]. The EMR of the studied system is represented in Fig. 1*b*. Moreover, EMR enables a deduction of control schemes by an inversion principle. The vehicle control can then be defined. The driver acts as a closed-loop controller of the velocity v_{ev} to define the total reference force $F_{tot\text{-}ref}$ by acting on the acceleration and braking pedals:

$$F_{tot-ref} = C(t)\left(v_{ev-ref} - v_{ev-meas}\right) \tag{7}$$

with $C(t)$ a controller, which could be a neural network controller in the case of the driver. The total reference force $F_{tot\text{-}ref}$ is then distributed into the traction force reference $F_{trac\text{-}ref}$ and the mechanical braking force reference $F_{mb\text{-}ref}$ by an inversion of (4):

$$\begin{cases} F_{trac-ref} = k_D F_{tot-ref} \\ F_{mb-ref} = (1-k_D) F_{tot-ref} \end{cases} \tag{8}$$

with k_D a distribution input, which is defined by a strategy: $k_D=1$ in traction mode and k_D defined for a maximal electrical braking in braking mode ($0 \leq k_D \leq 1$). The reference of the drive torque $T_{ed\text{-}ref}$ is finally obtained by an inversion of (3):

$$T_{ed-ref} = \left(r_{wh} / k_g\right) F_{trac-ref} \tag{9}$$

2.2 Off-road method characterization

Let us assume that vehicle parameters are known, except the electric drive efficiency map. If the electric drive can be removed from the vehicle, it can be connected to a load electric drive and all tests can be run to define the efficiency map. A load machine is then connected to the shaft of the tested electric machine. Here, the off-road method corresponds to the method A of the IEEE 112 test procedure for electric machines [21] extended to tested electric drives [15]. Such a method requires speed control of the load electric drive and measurements of the voltage u_{dc}, current i_{ed}, rotation speed Ω_{ed} and torque T_{ed}. These variables correspond to the inputs and outputs of the electric drive model depicted by the EMR (orange circle in Fig. 1*b*). The efficiency is then derived from (2):

$$\eta_{ed}\left(T_{ed}, \Omega_{ed}\right) = \frac{P_{out}}{P_{in}} = \frac{T_{ed-meas}\Omega_{ed-meas}}{u_{dc-meas}\, i_{ed-meas}} \tag{10}$$

A look-up table is then built off-line by imposing different operating points to the tested electric drive. To build a matrix for the torque-speed plane, the tested drive is thereby controlled to impose the torque $T_{ed\text{-}ref}$ while the load electric drive is controlled to impose the rotation speed $\Omega_{ed\text{-}ref}$ (Fig. 2*a*). Consequently, all operating points can be covered by changing the reference values in the matrix $\{T_{ed\text{-}ref}, \Omega_{ed\text{-}ref}\}$. The finite number of the operating points recorded can afterward be extended to a continuous efficiency map by interpolation and extrapolation [36].

It should be noted that the off-road method assumes operation in steady-state to calculate the efficiency of each operating point, thus neglecting transient states. The measurements must then be carried out after the transient states. Furthermore the calculation of the efficiency requires the measurement of the torque. A torque sensor, which is generally expensive, is necessary. Another possibility is to use an estimator based on the parameters and measurement of the electric drive currents [37].

In the case of the electric drive characterization of a commercial EV, the use of the off-road method is not convenient. This method requires to remove the electric drive from the vehicle and install it on the test bed to be finally remounted in the vehicle with the risk of damage. To tackle this issue, an on-road method can been used to avoid the use of such an intrusive method.

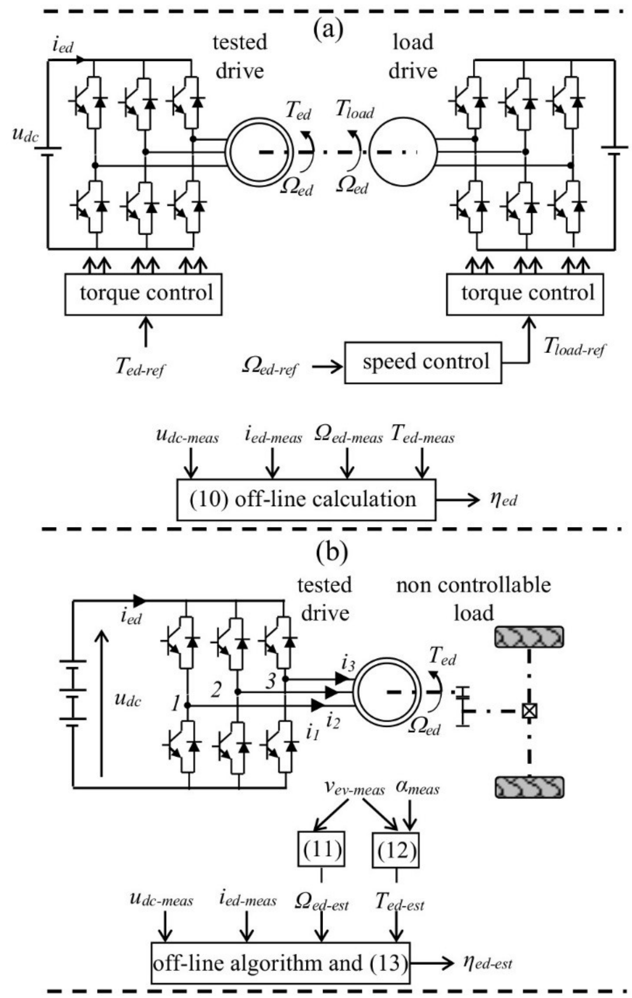

Fig. 2 *Methods to determine the efficiency map of an electric drive*
a Off-road method
b On-road method

2.3 On-road method characterization

A new on-road method has been proposed in [28] to determine an efficiency map using a real on-road driving cycle. Two issues have to be solved to determine the efficiency map. First, all the required measurements are generally not available, such as the torque of the electric drive. Second, steady-state operating points are not imposed by an on-road drive cycle and do not span the full torque-speed plane.

In the vehicle, only global sensors can be implemented without major changes (non-intrusive measurements). The measurements of the battery voltage and current can be easily integrated. The measurements of the rotation speed and of the torque of the electric machine cannot be implemented as easily. A GPS (Global Positing System) is a widely used non-intrusive sensor that provides the vehicle position and altitude, which can be converted into the vehicle velocity v_{ev} and slope α. These available measurements are not close to the mechanical input and output of the electric drive, Ω_{ed} and T_{ed}.

A first issue of the on-road method is to estimate the rotation speed and torque of the electric drive from the available measurements (Fig. 2*b*). From (3) the rotation speed can be estimated using the measurement of the velocity:

$$\Omega_{ed-est} = \left(k_g / r_{wh}\right) v_{ve-meas} \tag{11}$$

As in general the braking strategy of commercial vehicles is not well-known by the users, only the traction mode is studied. The efficiency map will be then studied in the first quadrant of the torque-speed plane. In traction mode, from (3), (5) and (6) the drive torque T_{ed} can be estimated using the measurements of the velocity v_{ev} and slope angle α:

$$T_{ed-est} = \frac{r_{wh}}{\eta_g^k k_g}\left[M\left(\frac{dv_{ev}}{dt}\right) + 0.5pAC_x v_{ev-meas}^2 + Mg\left(\sin\alpha_{meas} + f_r\right)\right] \tag{12}$$

This estimation requires the derivative of the velocity that leads to an approximation. Using estimations, $\Omega_{ed\text{-}est}$ and $T_{ed\text{-}est}$, the efficiency of the electric drive can be defined using the measurements of the battery voltage u_{dc} and current i_{ed}:

$$\eta_{ed-est}\left(T_{ed-est},\Omega_{ed-est}\right)=\frac{P_{out-est}}{P_{in-est}}=\frac{T_{ed-est}\Omega_{ed-est}}{u_{dc-meas}i_{ed-meas}} \tag{13}$$

A second issue of the on-road method is the available operating points during the on-road drive cycle. Because of the dynamical nature of the identification process, the torque-speed data points are recorded in an unorderly fashion, with unevenly distributed data and unexplored regions in the plane. The drive cycle has to be as varied as possible to obtain operating points that cover large areas of the torque-speed plane. An off-line algorithmic method was proposed in [28] to obtain a complete efficiency map, with uniformly distributed data points from the recorded data (estimated torque $\underline{T}_{ed\text{-}est}$ and speed $\underline{\Omega}_{ed\text{-}est}$ data vectors and resulting efficiency $\underline{\eta}_{ed\text{-}est}$) following the following main steps:

1. round the data according to the desired quantization for velocity and torque points on the grid;
2. sort the data, averaging efficiency for repeated points;
3. remove outliers;
4. fill gaps in the map by using linear interpolation;
5. complete the borders of the map by setting the efficiency to the same value as the estimated efficiency at the last points of the map.

The on-road method has been applied to a commercial EV, the Tazzari Zero [29] (Fig. 1*c*, Table 2). The vehicle, propelled by an induction machine of 15 kW, has been instrumented with sensors of the battery voltage and current as well as a GPS antenna with a velocity accuracy of 0.1 m/s. An on-board acquisition system (CompactRIO, National Instrument) acquires the data every 0.5 s. The acquisition system is powered by two additional lead-acid batteries (12 V, 17.5 Ah). The power consumption of the acquisition system then does not alter the energy flow of the EV.

Table 2. *Electric vehicle parameters*

parameter	value
gearbox ratio k_{gb}	5.84
gearbox efficiency η_{gb}	0.98
wheels radius r_{wh} [m]	0.2865
curb mass [kg]	562
$A\cdot C_x$ [m^2]	0.7
f_r	0.02

An extra-urban drive cycle has been carried out at University of Lille 1, in France, on and around campus. The measurements are recorded by the on-board acquisition system: battery voltage u_{dc}, battery current i_{ed}, vehicle velocity v_{ev}, and altitude (blue curves in Fig. 3*a*). The velocity reaches a maximum of 80 km/h (22 m/s). From that data, parameters of Table 2 and the measured slope α_{meas} are implemented off-line in (12) to define the estimated torque $T_{ed\text{-}est}$. The rotation speed Ω_{ed} is estimated off-line using (11). The efficiency is then calculated for each operating point using (13). A first efficiency map has been built for the operating points of the driving cycle (Fig. 3*b*). It should be noted that the operating points cover most of the torque-speed plane. It could be improved by a more adapted drive cycle, which can be studied in further works. From the initial efficiency map, the off-line algorithm of [28] is used to obtain the final efficiency map (Fig. 3*c*). This on-road efficiency map can then be used in simulation.

Simulation results with the obtained efficiency map of Fig. 3*c* show some dynamical errors in comparison with the experimental results (Fig. 3*a*). The average error of the current of the machine is 2 % on the duration of the driving cycle. In term of energy consumption less than 3.5 % average error is yielded.

In the on-road method, operating points and the dynamic conditions are influenced by the driver behaviors. Fig. 4 presents the electric drive efficiency map of the Tazzari Zero, deduced from two different driving cycles. It should be noted that the obtained efficiency maps are similar to the previous one (Fig. 3*c*). The absolute difference of the efficiency maps from (*a*) and (*b*) is presented in (*c*). The global average difference is 2.4 % for a standard deviation of 1.79 %, what means that both efficiency maps are quite similar. The on-road method is then repeatable and applicable for any instrumented vehicle.

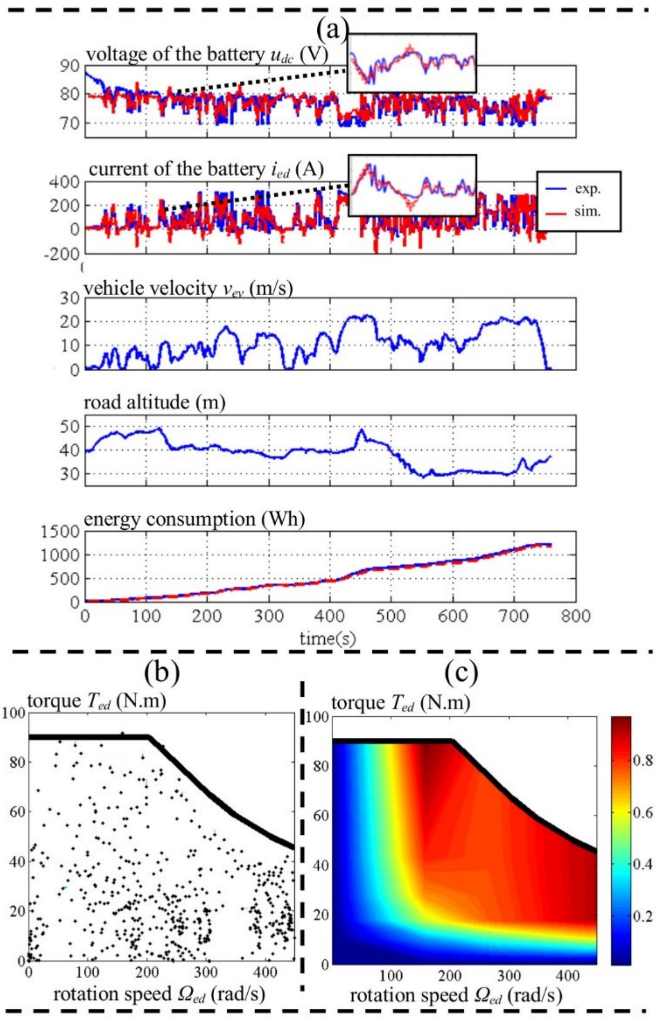

Fig. 3 *Results for the on-road method*

a Experimental and simulation results
b On-road test operating points of the efficiency map
c Final on-road efficiency map after processing

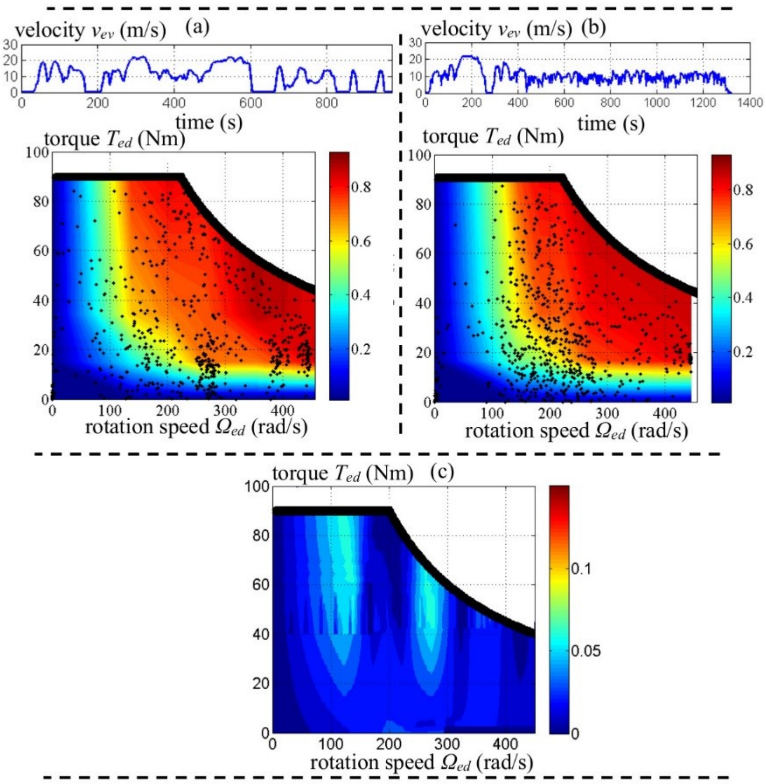

***Fig. 4**: On-road efficiency maps of the studied electric vehicle for different driving cycles*
a efficiency map of the driving cycle 1
b efficiency map of the driving cycle 2
c absolute difference between efficiency maps of the driving cycles 1 and 2

3 Application to a Versatile Experimental Setup

To compare in an effective way both methods a versatile experimental setup is necessary. This setup has to be capable to test both methods with the same platform. The experimental setup is then composed of a Voltage-Source-Inverter (VSI) and an induction machine under test connected to a load electric machine with its own VSI. For the on-road method the load electric drive is controlled by a Hardware-In-the-Loop (HIL) simulation technique [38] to emulate the mechanical part of the vehicle. For the off-road method the load electric drive is controlled to impose the rotation speed. The on-road efficiency map can consequently be compared to the off-road efficiency map with the same experimental setup.

3.1 Experimental setup

A 20 kW induction machine, its VSI and its torque control are considered as the tested electric drive (Fig. 5*a*). The load electric drive is composed of a 20 kW permanent magnet synchronous machine, its VSI and its torque control. A 1005 dSPACE controller board is used with a sampling period of T_{samp}=100 µs and a switching frequency of f_{sw}=10 kHz.

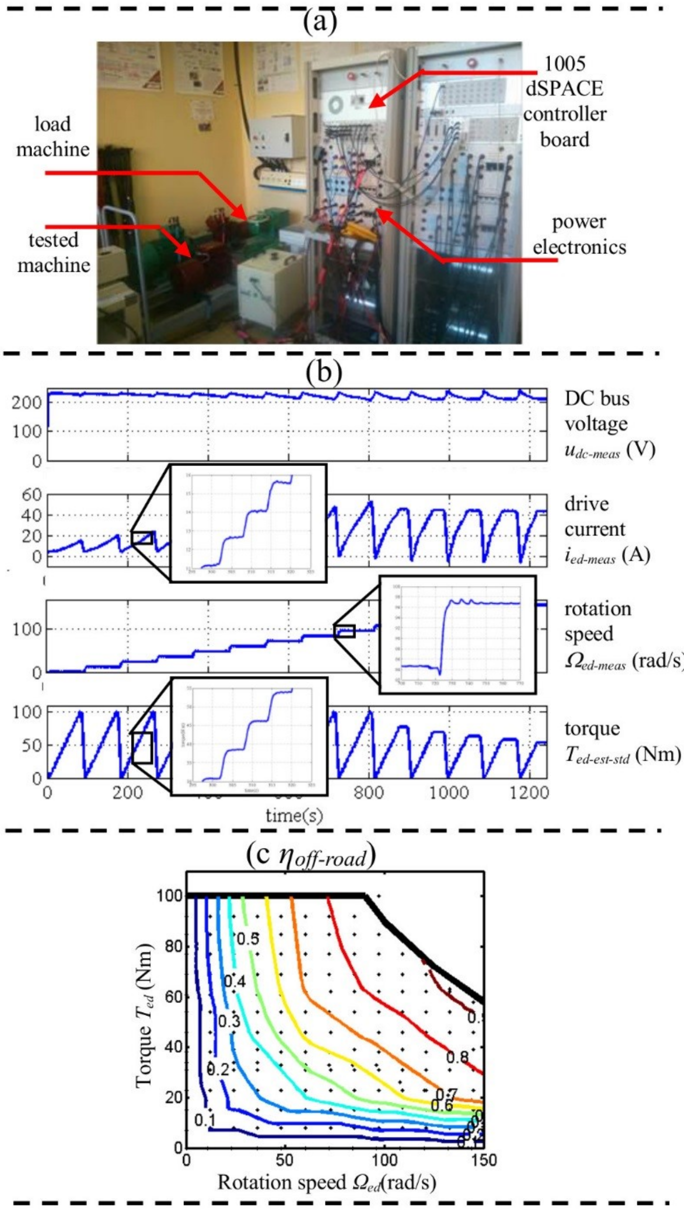

Fig. 5 *Off-road method applied on the versatile experimental setup*

a Versatile experimental setup
b Experimental results of the electric drive
c Off-road efficiency map of the electric drive

Both electric machines are connected by a common shaft. The rotation speed Ω_{ed} is a function of the tested electric drive and load torques, T_{ed} and T_{load}:

$$J\frac{d}{dt}\Omega_{ed} = T_{ed} - T_{load} - f\Omega_{ed} \tag{14}$$

where J and f are the inertia and friction coefficient of the shaft. To impose the rotation speed $\Omega_{ed\text{-}ref}$ to the load electric drive (see Fig. 2*a*), the load torque reference $T_{load\text{-}ref}$ is determined by an inversion of (14):

$$T_{load-ref} = C_{\Omega}(t)\left(\Omega_{ed-ref} - \Omega_{ed-meas}\right) \tag{15}$$

with $C_{\Omega}(t)$ the speed controller. Classical field oriented control is used for both electric drives to set their torque references [39]. The rotation speed Ω_{ed} and torque T_{ed} can then be imposed to the tested electric drive. Because there is no torque sensor on the experimental setup, the torque of the tested electric drive is estimated from the classical relation using the measurement of the currents and rotation speed of the tested induction machine [37]:

$$T_{ed-est-std} = p\frac{M_{sr}}{L_r}\phi_{rd-est}i_{sq-est} \text{ with } \phi_{rd-est}, i_{sq-est} = f\left(\underline{i}_{1,2-meas}, \Omega_{ed-meas}\right) \tag{16}$$

where L_r is the rotor inductance of the induction machine, M_{sr} the mutual inductance between the stator and rotor, p the pole pair number, ϕ_{rd} the d-axis rotor flux, i_{sq} the q-axis stator current and $\underline{i}_{1,2}$ the electric machine current vector. This estimation has been shown to have a good correlation with the measured electric drive torque [37].

3.2 Off-road efficiency map

The standard IEEE 112 procedure [21] is extended to the electric drive [15] to determine the off-road efficiency map. Different operating points are imposed to the tested drive with a 14×14 matrix for the torque-speed plane. Rotation speed steps of 12 rad/s are imposed from 0 to 157 rad/s ($\Omega_{ed\text{-}ref}$). For each value of rotation speed, torque steps of 7.7 Nm are imposed from 0 to 100 Nm ($T_{ed\text{-}ref}$, Fig. 5*b*). For each operating point, the measurements are carried out in steady-state (black dots in Fig. 5*c*). The number of operating points has been defined to give enough points to construct an efficiency map of high quality without relying too much on interpolation.

The efficiency map is then calculated using (13) from the measurements of the dc bus voltage $u_{dc\text{-}meas}$, electric drive current $i_{ed\text{-}meas}$, rotation speed $\Omega_{ed\text{-}meas}$ and the estimation of the torque $T_{ed\text{-}est\text{-}std}$ (Fig. 5*b*) using (16). The torque-speed plane is composed of regularly spaced operating points, and iso-efficiency lines can be plotted (Fig. 5*c*).

3.3 On-road efficiency map

To reproduce the on-road method on the experimental setup, the rotation speed and torque references are imposed using a power HIL simulation of the vehicle (Fig. 6*a*). Power HIL simulation [38] is more and more used to test Electronic Control Unit (ECU) and power components before their implementation in an actual system. EMR is a useful tool to organize HIL simulation. It has often been used for the description of HIL simulation for electric and hybrid vehicles [35], [40].

In our case, the estimated torque $T_{ed\text{-}est\text{-}std}$ of the tested electric drive is sent to mathematical model of the mechanical transmission and deduced from the EMR of Fig. 1*b* (purple part in Fig. 6*b*). This torque estimation is defined from the current and speed measurements (16) to be as close as possible to the real torque. From interactions between all models of mechanical components, the rotation speed is generated ($\Omega_{ed\text{-}ref}$ in Fig. 6*b*). This rotation speed is used as a reference for the speed control of the load electric drive. Moreover, the vehicle control defines the torque reference of the tested electric drive $T_{ed\text{-}ref}$. The model of the vehicle, control of the vehicle and controls of both electric drives are computed in real time on a 1005 dSPACE controller board. In comparison with the off-road method, the rotation speed and torque references are not defined by steps, but by the dynamical behaviour of the simulated vehicle with its model and control (as in the real vehicle).

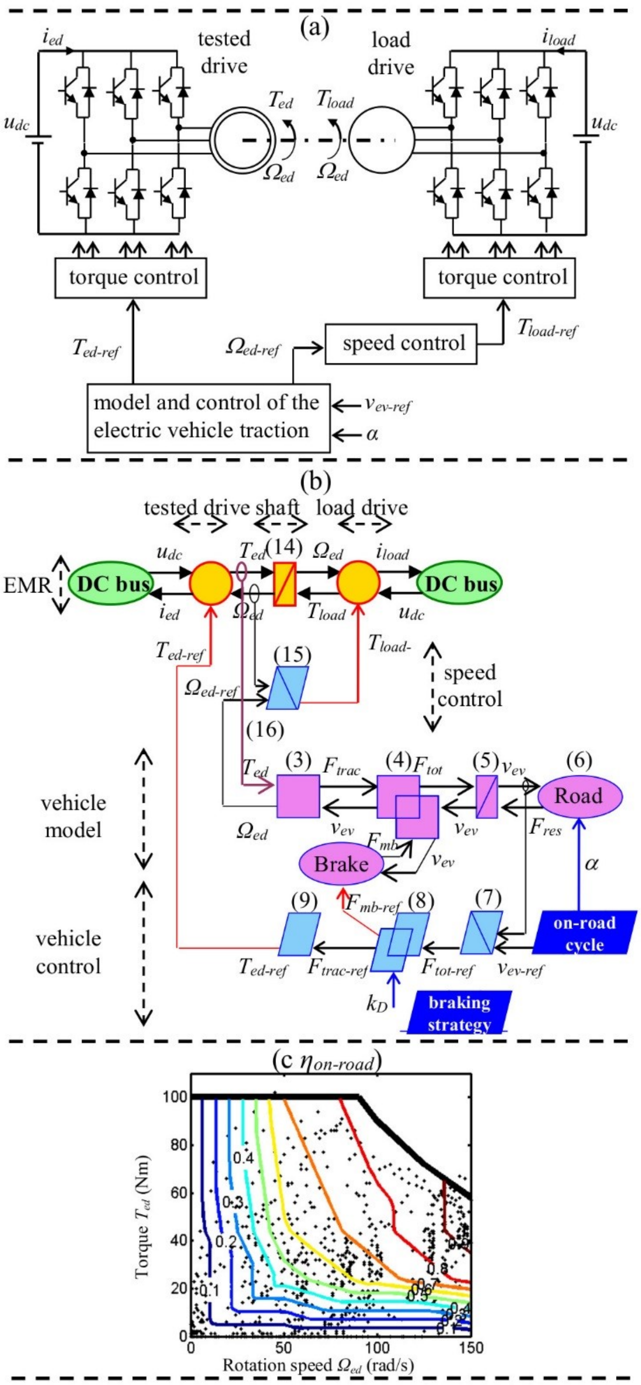

Fig. 6 *On-road method applied on the versatile experimental setup*

a Power HIL simulation of the studied electric vehicle
b EMR and control of the power HIL simulation
c On-road efficiency map of the electric drive

The measurement of the velocity v_{ev} of the on-road drive cycle of the EV Tazzari Zero, see Fig. 3*a*, is imposed as a reference to the vehicle control ($v_{ev\text{-}ref}$ in Fig. 6*b*). The measurement of the altitude, see Fig. 3*a*, is imposed to the road model to determine the slope α (“Road” element in Fig. 6*b*). The on-road drive cycle is thus reproduced to the experimental setup. The efficiency map is built in the same way than for the EV with the measurements of the dc bus voltage u_{dc}, drive current i_{ed}, vehicle velocity v_{ev} and also the estimation of the torque T_{ed} using (12) with the vehicle velocity and road slope. The on-road efficiency map (Fig. 6*c*) is relatively close to the off-road efficiency map (Fig. 5*c*), even though it is obtained from transient operation.

4 Comparison of the Methods

The on-road and off-road methods do not use the same procedure to determine the efficiency map of an electric drive of an EV. Different assumptions and approximations are considered for both methods. First, the electrical torque is estimated in a different way. The electrical torque is estimated from the velocity measurement in the on-road method while it is estimated from the measurement of the current in the off-road method. Second, the efficiency map is built in transient states for the on-road method whereas it is built in steady-state for the off-road method. Other errors occur due to the sensor accuracies, but they do not have to be considered because the sensors are the same for the on-road and off-road methods during the tests on the experimental setup.

4.1 Differences of the efficiency maps

To further validate the efficiency map of both on-road and off-road methods a measurements with a new driving cycle, different from the one that has been used to determine the efficiency map of Fig. 6*c*, has been performed (Fig. 7). The efficiency maps are then tested with other operating points. For the on-road method, the comparison between experimental and simulation results gives an average error of 1.7 % for the current and 1.9 % for the energy consumption. For the off-method, an average error of 0.35 % for the current and 0.3 % for the energy consumption is obtained. The high accuracy between experimental and simulation results allows to validate the obtained efficiency maps. Both methods are then validated.

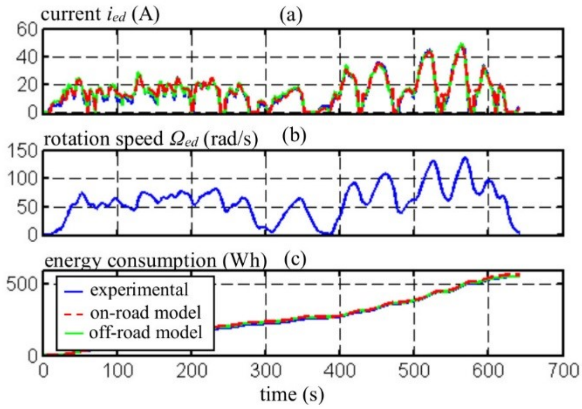

Fig. 7 *Validation of the efficiency maps of both on-road and off-road methods on a new driving cycle*

To compare the efficiency maps of each method, the difference between the two maps is calculated as follows and plotted in Fig. 8*a*.

$$difference = |\eta_{\text{off-road}} - \eta_{\text{on-road}}| \tag{17}$$

Two areas can be considered (Fig. 8*a*). In area 1 the average difference of the efficiencies is 3 % with a maximal difference of 6 %. In this area, the on-road efficiency map can be considered accurate enough to represent the electric drive for energetic studies. In area 2, at low torques and high speeds, the average difference is 10 % with a maximal difference of 14 %. The area with the highest difference corresponds simultaneously to a region with few operating points for the on-road method (black dots in Fig. 8*a*), and with a large gradient of efficiency about torque. The global average difference, with areas 1 and 2, is 3.3 % for a standard deviation of 3.15 %, what means that 68% of values fall within 1 standard deviation of the average. All the comparison results are summarized in Table 3. The effects of torque estimation and of transient states are evaluated in the next subsections.

4.2 Influence of the torque estimation

In the on-road method, the estimation of the torque is achieved from the derivation of the velocity measurement using the mechanical load model (12). In the off-road method the estimation of the torque is carried out using the measurements of the current and the rotation speed using the electromagnetic model of the motor (16).

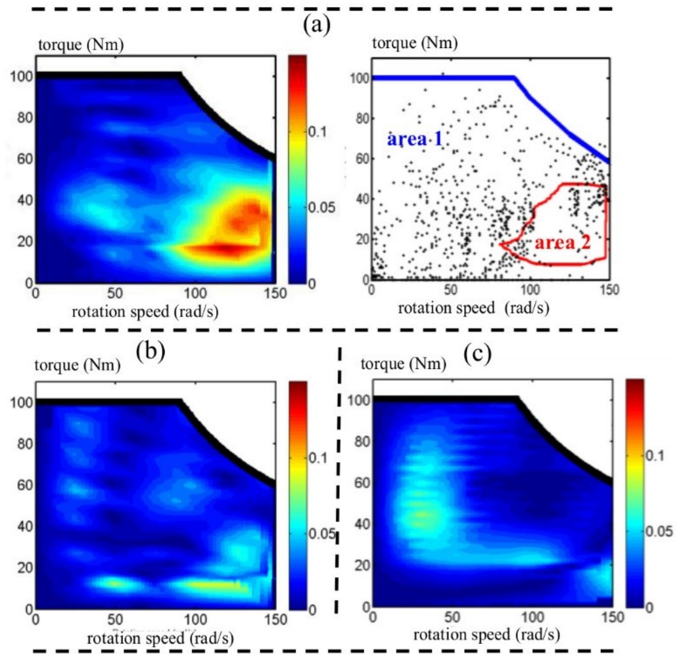

Fig. 8 *Absolute difference between efficiency maps*
a Original on-road versus off-road method
b On-road method with electromagnetic torque estimation versus original off-road method
c Off-road method with torque ramp profile versus original off-road method

Another on-road efficiency map is built from the on-road method. (Fig. 8*b*) To avoid the derivation of the measurement of the velocity the electromagnetic torque estimation (16) is then used. For this test only the torque estimation for the on-road method has been changed. The characterization is still the same with a building of the efficiency map in transient states for the on-road method and in steady-state for the off-road method. When comparing Fig. 8*a* and Fig. 8*b*, the use of the electromagnetic torque (16) leads to a smaller absolute difference on the overall plane, except for some isolated regions. It should be noted that these regions correspond to areas of the plane with gaps in experimental data points (black dots on Fig. 8*a*). The maximum difference on area 2 of Fig. 8*b* has been significantly reduced down from 14 % to 8 %. It can be concluded that torque estimation plays an important role in efficiency estimation and that it accounts for a large portion of the difference in area 2. More accurate torque estimation, such as closed loop observation, could improve the results of the on-road efficiency map. The average difference is 2.2 % with a standard deviation of 1.76 % (Table 3).

4.3 Influence of the transient states

To measure the impact of the transient states, the off-road method is modified to use measurements during transients: instead of imposing torque steps and waiting for steady-state, a ramp is used for the reference torque. A new efficiency map is then built and compared to the efficiency map obtained with the original off-road method of Fig. 5*b* (Fig. 8*c*). For this test only the reference torque of the off-road method has been changed. The torque estimation does not change: derivation of the velocity for the on-road method and measurements of the machine current for the off-road method.

A maximal difference of 6% is concentrated for low rotation speeds with medium torques (Fig. 8*c*). Overall, the use of transient states represents only a difference of efficiency of 2% and is not the main factor for the accuracy of the results. It can be concluded that the transient measurements affect the efficiency estimation, but play a minor role as compared to lack of measurement points and quality of torque estimation. The average difference is 2.15 % with a standard deviation of 1.18 % (Table 3).

Table 3. Statistical analysis differences

Comparison	On-road vs off-road	Influence of the torque estimation	Influence of the transient states
Average difference	3.33 %	2.2 %	2.15 %
Standard deviation	3.15 %	1.76 %	1.18 %

5 Conclusion

Two methods to determine the efficiency map of the electric drive of EVs have been compared experimentally. An off-road method allows determining the efficiency map with a dedicated experimental test bed. This standard method is accurate, but suffers from application constraints. An on-road method allows determining the efficiency map directly in-vehicle by an on-road drive cycle. The on-road method is repeatable and convenient to use but, as it is a new method, its reliability is unknown. To compare in an effective manner both methods, a versatile experimental setup has been used. To reproduce the behaviour of the EV, a power Hardware-In-the-Loop simulation technique has been used. By this way, the on-road efficiency map has been compared with the map obtained with the off-road method. It has been shown that, in an energetic point of view, both methods yield similar results. Our comparison demonstrates an absolute difference of the efficiency lower than 6% in most of the torque-speed plane. The principal differences come from the lack of measurement points for the on-road method due to the on-road driving cycle. The quality of torque estimation also affects the results. Furthermore, the efficiency map is built in transient states for the on-road method whereas it is built in steady-state for the off-road method. The experimental results show that the transient nature of measurements has a minor influence on the map accuracy as compared to lack of measurement points and quality of torque estimation. For the benchmarking of commercial vehicle, as it is not necessary to remove the electric drive from the vehicle, the on-road method can be more efficient, gains research time, and avoids the risk of damage. The new on-road method can then be used for energetic studies. For future work, more accurate torque estimation is required to increase the accuracy of the on-road efficiency map in sensitive areas. Furthermore, the new on-road method could be used to compare different commercial EVs.

6 References

[1] Chan, C.C.: 'Overview of Electric, Hybrid and Fuel Cell Vehicles', in Crolla, D. (Ed.): 'Encyclopedia of Automotive Engineering' (Wiley-Blackwell, 2015), pp. 971-974

[2] Zhong, F., Martinez, O., Gormus, R., *et al.*: 'The reign of EV's? An economic analysis from consumer's perspective', *IEEE Electrification Magazine*, 2014, **2**, (2), pp. 61-71

[3] Khaligh, A., Li, Z.: 'Battery, ultracapacitor, fuel cell, and hybrid energy storage systems for electric, hybrid electric, fuel cell, and plug-in Hybrid Electric Vehicles: state-of-the-art', *IEEE Trans. on Vehicular Technology*, 2010, **59**, (6), pp. 2806-2814

[4] Ehsani, M., Gao, Y., Gay, S.E., *et al.*: 'Modern electric, hybrid electric, and fuel cell vehicles' (CRC Press, 2009, 2nd edn.)

[5] Gao, D.W., Mi, C., Emadi, A.: 'Modeling and simulation of electric and hybrid vehicles', *Proceedings of the IEEE*, 2007, **95**, (4), pp. 729–745

[6] Guzzella, L., Sciarretta, A.: 'Vehicle propulsion systems, introduction to modelling and optimization' (Springer-Verlag Berlin and Heidelberg GmbH & Co, 2015, 3rd edn.)

[7] Lee, B., Lee, S., Cherry, J., *et al.*: 'Development of advanced light-duty powertrain and hybrid analysis tool', SAE 2013 World Congress & Exhibition, 2013

[8] Vinot, E., Trigui, R., Cheng, Y., *et al.*: 'Improvement of an EVT-based HEV using dynamic programming', *IEEE Trans. on Vehicular Technology*, 2014, **63**, (1), pp. 40-50

[9] Lazari, P., Wong, J., Chen, L.: 'A computationally efficient design technique for electric-vehicle traction machines', *IEEE Trans. on Industry Applications*, 2014, **50**, (5), pp. 3203-3213

[10] Jurkovic, S., Rahman, K.M., Morgante, J.C., *et al.*: 'Induction machine design and analysis for general motor e-assist electrification technology', *IEEE Trans. on Industry Applications*, 2015, **51**, (1), pp. 631-639

[11] Patil, R.M., Filipi, Z., Fathy, H.K.: ‘Comparison of supervisory control strategies for series plug-in hybrid electric vehicle powertrains through dynamic programming’, *IEEE Trans. on Control Systems Technology*, 2014, **22**, (2), pp. 502-509

[12] Mayet, C., Pouget, J., Bouscayrol, A., *et al.*: ‘Influence of an energy storage system on the energy consumption of a diesel-electric locomotive’, *IEEE Trans. on Vehicular Technology*, 2014, **63**, (3), pp. 1032-1040

[13] Chan, C.C., Bouscayrol, A., Chen, K.: ‘Electric, hybrid and fuel cell vehicles: architectures and modeling’, *IEEE Trans. on Vehicular Technology*, 2010, **59**, (2), pp. 589-598

[14] Buyukdegirmenci, V.T., Bazi, A.M., Krein, P.T.: ‘Evaluation of induction and PM synchronous machines using drive-cycle energy and loss minimization in traction application’, *IEEE Trans. on Industry Applications*, 2014, **50**, (1), pp. 395-403

[15] Estima, J.O., Marques Cardoso, A.J.: ‘Efficiency analysis of drive train topologies applied to electric/hybrid vehicles’, *IEEE Trans. on Vehicular Technology*, 2012, **61**, (3), pp. 1021-1031

[16] Williamson, S.S., Lukic, S.M., Emadi, A.: ‘Comprehensive drive train efficiency analysis of hybrid electric and fuel cell vehicles based on motor-controller efficiency modelling’, *IEEE Trans. on Power Electronics*, 2006, **21**, (3), pp. 730–740

[17] Cao.W: ‘Comparison of IEEE 112 and new IEC standard 60034-2-1’, *IEEE Trans. on Energy Conversion*, 2009, **24**, (3), pp. 802-808

[18] Moskalik, A., Dekraker, P., Kargul, J., *et al.*: ‘Vehicle component benchmarking using a chassis dynamometer’, *SAE International Journal of Materials and Manufacturing*, 2015, **8**, (3), pp. 869-879

[19] Bojoi, R., Armando, E.,Pastorelli, M., Lang, K.: ‘Efficiency and loss mapping of AC motors using advanced testing tools’, *2016 XXII International Conference on Electrical Machines (ICEM)*, 2016

[20] Boglietti. A, Cavagnino. A, Lazzari. M, Pastorelli. M.: ‘International standards for the induction motor efficiency evaluation: a critical analysis of the stray-load loss determination’, *IEEE Trans. on Industry Applications*, 2004, **40**, (5), pp. 1294-1301

[21] IEEE Std 112-1996: ‘IEEE standard test procedure for polyphase induction motors and generators’, 1997

[22] IEC 60349-2: ‘Electric traction – rotating electrical machines for rail and road vehicles – Part 2: Electronic converter-fed alternating current motors’, 2010.

[23] CSA Std C390-93: ‘Energy efficiency test methods for three-phase induction motors’, 1993.

[24] Wang, R., Chen, Y., Feng, D., *et al.*: ‘Development and performance characterization of an electric ground vehicle with independently actuated in-wheel motors’, *Journal of Power Sources*, 2011, **196**, (8), pp. 3962-3971

[25] Kim, S., Park, S., Park, T., *et al.*: ‘Investigation and experimental verification of a novel spoke-type ferrite-magnet motor for electric-vehicle traction drive applications’, *IEEE Trans. on Industrial Electronics*, 2014, **61**, (10), pp. 5763-5770

[26] Bohn, T., Duoba, M.: ‘Implementation of a non-intrusive in-vehicle engine torque sensor for benchmarking the Toyota Prius’, SAE 2005 World Congress & Exhibition, 2005

[27] Irimescu, A., Mihon, L., Pãdure, G.: ‘Automotive transmission efficiency measurement using a chassis dynamometer’, *International Journal of Automotive Technology*, 2011, **12**, (4), pp. 555-559

[28] Dépature, C., Lhomme, W., Bouscayrol, A., *et al.*: ‘Efficiency map of the traction system of an electric vehicle from an on-road test drive’, 2014 IEEE Vehicle Power and Propulsion Conf. (VPPC), 2014

[29] ‘Tazzari zero website’, http://www.tazzari-zero.com/, accessed 8 August 2016

[30] Letrouvé, T., Bouscayrol, A., Lhomme, W., *et al*: 'Different models of a traction drive for an electric vehicle simulation', 2010 IEEE Vehicle Power and Propulsion Conf. (VPPC), 2010

[31] Bouscayrol, A., Hautier, J.P., Lemaire-Semail, B.: 'Graphic formalisms for the control of multi-physical energetic systems: COG and EMR', in Roboam, X. (Ed.): 'Systemic design methodologies for electrical energy systems: analysis, synthesis and management' (John Wiley & Sons, 2012)

[32] Castaings, A., Lhomme, W., Trigui, R., *et al.*: 'Practical control schemes of a battery/supercapacitor system for electric vehicle', *IET Electr. Syst. Transp.*, 2016, **6**, (1), pp. 20-26

[33] Lhomme, W., Trigui, R., Delarue, P., *et al.*: 'Switched causal modelling of transmission with clutch in hybrid electric vehicles', *IEEE Trans. on Vehicular Technology*, 2008, **57**, (4), pp. 2081-2088

[34] Allègre, A.-L., Bouscayrol, A., Trigui, R.: 'Flexible real-time control of a hybrid energy storage system for electric vehicles', *IET Electr. Syst. Transp.*, 2013, **3**, (3), pp. 79–85

[35] Letrouvé, T., Lhomme, W., Bouscayrol, A., *et al.*: 'Control validation of Peugeot 3∞8 Hybrid4 vehicle using a reduced-scale power HIL simulation', *Journal of Electrical Engineering and Technology*, 2013, **8**, (5), pp. 1227-1233

[36] Deprez, W., Lemmens, J., Vanhooydonck, D., et al.: 'Iso-efficiency contours as a concept to characterize variable speed drive efficiency', 2010 International Conf. on Electrical Machines (ICEM), 2010

[37] Bastiaensen, C., Deprez, W., Symens, W., *et al.*: 'Parameter sensitivity and measurement uncertainty propagation in torque-estimation algorithms for induction machines', *IEEE Trans. on Instrumentation and Measurement*, 2008, **57**, (12), pp. 2727-2732

[38] Bouscayrol, A.: 'Hardware-in-the-loop simulations', in Wilamowski, B.M., Irwin, J.D. (Ed.): 'The Industrial Electronics Handbook' (CRC Press, 2011, 2nd edn.)

[39] Sul, S.K.: ‘Control of electric machine drive systems’ (Wiley-IEEE Press, 2011)

[40] Allègre, A.L., Bouscayrol, A., Verhille, J.N., *et al.*: ‘Reduced-scale-power hardware-in-the-loop simulation of an innovative subway’, *IEEE Trans. on Industrial Electronics*, 2010, **57**, (4), pp. 1175-1185

7 APPENDIX

Table 4. Nomenclature of variables

A	Frontal area [m^2]	R	Electric resistance [Ω]
C_x	Air drag coefficient [-]	SoC	State of charge [%]
f_r	Rolling resistance [-]	T	Torque [Nm]
F	Force [N]	u	Electric voltage [V]
g	Grav. acceleration [m/s^2]	v	Velocity [m/s]
i	Electric current [A]	α	Slope [%]
k	Constant ratio [-]	Ω	Angular speed [rad/s]
M	Vehicle mass [kg]	η	Efficiency [%]
P	Power [W]	ρ	Air density [kg/m^3]
r	Wheel radius [m]		

Table 5. Nomenclature of captions

0	Open voltage	m	Mechanical
bat	Battery	meas	Mesured variable
dc	Direct voltage	ref	Reference variable
ed	Electric drive	res	Mechanical resistance
est	Estimated variable	std	Standard
ev	Electric vehicle	tot	Total
gb	Gearbox	trac	Traction
load	Load machine	wh	Wheel
mb	Mechanical brake		

Table 6. Pictograms of Energetic Macroscopic Representation (EMR)

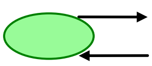	Source element (energy source)	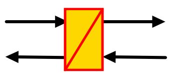	Accumulation element (energy storage)	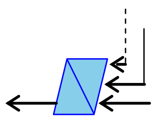	Indirect inversion (closed-loop control)
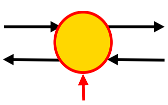	Multi-domain conversion element	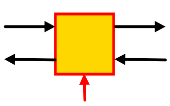	Mono-domain conversion element	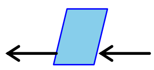	Direct inversion (open-loop control)
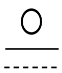	Sensor Mandatory Optional	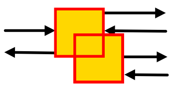	Mono-physical coupling element (energy distribution)	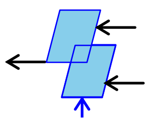	Coupling inversion (energy criteria)